CPEB3 inhibits translation of mRNA targets by localizing them to P bodies

Lenzie Ford[a,b,c,1], Emi Ling[a,d,1], Eric R. Kandel[a,b,c,e,2], and Luana Fioriti[a,f,2]

[a]Department of Neuroscience, Columbia University, New York, NY 10027; [b]Mortimer B. Zuckerman Mind Brain Behavior Institute, Columbia University, New York, NY 10027; [c]Howard Hughes Medical Institute, Chevy Chase, MD 20815; [d]Department of Genetics, Harvard Medical School, Broad Institute of MIT and Harvard, Cambridge, MA 02142; [e]Kavli Institute for Brain Science, Columbia University, New York, NY 10027; and [f]Dulbecco Telethon Institute, Istituto di Ricerche Farmacologiche Mario Negri, 20156 Milan, Italy

Contributed by Eric R. Kandel, June 28, 2019 (sent for review September 20, 2018; reviewed by Cristina M. Alberini and Sathyanarayanan V. Puthanveettil)

Protein synthesis is crucial for the maintenance of long-term memory-related synaptic plasticity. The cytoplasmic polyadenylation element-binding protein 3 (CPEB3) regulates the translation of several mRNAs important for long-term synaptic plasticity in the hippocampus. In previous studies, we found that the oligomerization and activity of CPEB3 are controlled by small ubiquitin-like modifier (SUMO)ylation. In the basal state, CPEB3 is SUMOylated; it is soluble and acts as a repressor of translation. Following neuronal stimulation, CPEB3 is de-SUMOylated; it now forms oligomers that are converted into an active form that promotes the translation of target mRNAs. To better understand how CPEB3 regulates the translation of its mRNA targets, we have examined CPEB3 subcellular localization. We found that basal, repressive CPEB3 is localized to membraneless cytoplasmic processing bodies (P bodies), subcellular compartments that are enriched in translationally repressed mRNA. This basal state is affected by the SUMOylation state of CPEB3. After stimulation, CPEB3 is recruited into polysomes, thus promoting the translation of its target mRNAs. Interestingly, when we examined CPEB3 recombinant protein in vitro, we found that CPEB3 phase separates when SUMOylated and binds to a specific mRNA target. These findings suggest a model whereby SUMO regulates the distribution, oligomerization, and activity of oligomeric CPEB3, a critical player in the persistence of memory.

cytoplasmic polyadenylation | P bodies | SUMO | neurons | phase separation

A key feature of memory storage is synaptic plasticity, the ability of synapses to change their strength in response to activity (1). Because the maintenance of long-term memory requires new protein synthesis, this form of memory is highly linked with translational regulation. Among these regulators of translation, one group that is particularly important is the cytoplasmic polyadenylation element-binding protein (CPEB) family of proteins that includes several RNA-binding proteins associated with translational control. In mice, four CPEB proteins (named CPEB1 to 4) are expressed in the hippocampus, where new memories are formed (2, 3). Indeed, we found that one member of the CPEB family, CPEB3, is necessary for the maintenance of long-term memory storage (4). This protein is up-regulated following memory and following stimuli evoking long-term potentiation (LTP), a molecular mechanism thought to be important for memory storage. Following stimuli eliciting LTP, CPEB3 (3–6) exhibits a characteristic increase in oligomerization and in the promotion of mRNA translation (4–6). A glutamine-rich domain similar to those found in *Aplysia* CPEB and in yeast prions (3, 7, 8) exists in the N terminus of CPEB3, the proposed site that mediates oligomerization. Functionally, CPEB3 regulates the translation of mRNA targets, including AMPA-type glutamate receptor subunits GluA2 and GluA1, NMDA receptor subunit 1 (NR1), the cytoskeletal protein actin, and postsynaptic density protein 95 (PSD95) (4, 6, 9–11), all of which play major roles in synaptic plasticity (12–14). This regulation of translation of mRNA targets is connected to the structure of CPEB3. Soluble CPEB3 inhibits target mRNA translation while oligomeric, partially insoluble CPEB3 promotes the translation of target mRNA (4).

As neurons are polarized structures, we presume that mRNAs involved in the maintenance of long-term memory will be under strict spatial control. Indeed, intracellular transport of mRNA and local translation play a key role in neuronal physiology. Translationally repressed mRNAs are transported to distant dendritic sites as part of ribonucleoprotein (RNP) particles. A new class of RNP particles, the dendritic P body-like structures (dlPbodies), has been recently described (15). These P body-like structures are present in the soma and dendrites of mammalian neurons. These particles show motorized movements along dendrites and relocalize to distant sites in response to synaptic activation (15). Dcp1a, a critical component of these structures, is stably associated with dlP bodies in unstimulated cells, but exchanges rapidly upon neuronal activation, concomitant with the loss of Ago2 from dlP bodies. Thus, dlP bodies may regulate local translation by storing repressed mRNPs in unstimulated cells, and releasing them upon synaptic activation (15).

In the present study, we examine the subcellular localization of CPEB3 and identify one possible mechanism that explains how CPEB3 mediates the translation of its mRNA targets, namely by

Significance

Deciphering how cells regulate compartmentalization is critical for our understanding of local protein synthesis-dependent mechanisms, such as learning and memory. One way to achieve compartmentalization is by means of liquid–liquid phase separation, which results in the formation of membraneless organelles such as P bodies. In this study, we investigated how the cell regulates the inhibitory effect of the translation regulator cytoplasmic polyadenylation element-binding protein 3 (CPEB3), by means of small ubiquitin-like modifier (SUMO)ylation and localization to P bodies. Our findings on the role of SUMO as a critical mediator of CPEB3 phase separation might be relevant also in the context of the aberrant phase separation that characterizes other RNA-binding proteins implicated in neurodegenerative diseases, such as FUS (fused in sarcoma) and TDP-43 (TAR DNA binding protein 43) in ALS (amyotrophic lateral sclerosis).

Author contributions: L. Ford, E.L., and L. Fioriti designed research; L. Ford, E.L., and L. Fioriti performed research; L. Ford, E.L., and L. Fioriti analyzed data; and L. Ford, E.L., E.R.K., and L. Fioriti wrote the paper.

Reviewers: C.M.A., New York University; and S.V.P., The Scripps Research Institute.

The authors declare no conflict of interest.

[1]L. Ford and E.L. contributed equally to this work.

[2]To whom correspondence may be addressed. Email: erk5@columbia.edu or luana.fioriti@marionegri.it.

This article contains supporting information online at www.pnas.org/lookup/suppl/doi:10.1073/pnas.1815275116/-/DCSupplemental.

Published online August 15, 2019.

residing in P bodies under resting conditions and translocating to polysomes upon synaptic activity.

Results

CPEB3 Is Localized to the Nucleus and Enters the Cytoplasm via a Nuclear Export Signal. Previous studies primarily examined the cellular distribution of the CPEB3 protein within the mouse brain tissue (9, 16). To gain further insight into CPEB3's function, we studied its subcellular localization both within human cells (HeLa), which express CPEB3 endogenously (16), and within cultured neuronal cells. The *k*-nearest neighbor (k-NN) algorithm predicts that CPEB3 is widely distributed throughout the cell, mainly in the nucleus and cytosol. We tested this prediction experimentally using subcellular fractionation as described in Feng et al. (17), and found that CPEB3 distributes in most of the fractions analyzed, including fractions that contain important elements of the translational regulatory machinery such as the deadenylase CCR4 (18, 19) and the fragile X mental retardation protein (FMRP) (*SI Appendix*, Fig. S1). The distribution of CPEB3 in the same fraction of CCR4 is in agreement with previous studies in *Drosophila* of Orb, a CPEB ortholog (20). We also performed immunofluorescence experiments to confirm our biochemical fractionation experiments and confirmed that CPEB3-GFP and CCR4 colocalize (*SI Appendix*, Fig. S1). Our immunofluorescence analysis revealed that CPEB3-GFP appears to be both nuclear and cytoplasmic (*SI Appendix*, Fig. S1). Treatment with leptomycin, an antibiotic that blocks nuclear export, traps CPEB3-GFP in the nucleus, suggesting the presence of a nuclear export signal (NES) in CPEB3 (*SI Appendix*, Fig. S1) that is dependent on CRM1-mediated nuclear export (21).

To explore the possibility further, we analyzed the sequence of CPEB3 and found that it has a glutamine-rich, putative coiled-coil N-terminal domain (Nte) (8), two RNA recognition motifs (RRMs), and a C-terminal zinc finger (ZnF) domain (3). Sequence analysis tools predict that three putative NESs exist within the CPEB3 amino acid sequence: one within the disordered prion domain 2 (PrD2) region (6), one within RRM2, and another within the ZnF. The NES in PrD2 was indeed confirmed by Chao et al. (22), IPO5 being the specific karyopherin involved. However, Chao et al. show only a partial block in nuclear export of a CPEB3 lacking the NES in PrD2. This prompted us to test whether the predicted NESs in RRM2 and ZnF also contributed to the cytoplasmic shuttling of CPEB3. We transfected HeLa cells with either a full-length CPEB3-GFP or truncation mutants (*SI Appendix*, Fig. S1). We found that while CPEB3ΔRRM2-GFP still localized to the cytoplasm, CPEB3ΔZnF-GFP became trapped in the nucleus, suggesting that CPEB3 has a NES within the ZnF domain that is critical for nuclear export (*SI Appendix*, Fig. S1). These data suggest that there are two nuclear export signals on the CPEB3 sequence: one in PrD2, already identified by Chao et al., and one in the ZnF region, which also appears to contribute to CPEB3 shuttling to the cytosol.

CPEB3 Localizes to P Bodies in the Cytoplasm. In HeLa cells, transfected CPEB3-DsRed primarily localizes to the cytoplasm and displays both punctate and diffuse localization patterns. The shape, size, and distribution pattern of CPEB3-DsRed puncta resemble those of phase-separated, membraneless RNA granules such as processing bodies (P bodies) and stress granules (23) (*SI Appendix*, Fig. S1*A*). We utilized P-body and stress granule localization markers to identify which RNA granules CPEB3 resides in.

We first asked whether transfected CPEB3 colocalizes with three major mammalian P-body markers: Argonaute 2 (Ago2), GW182, and decapping 1 (Dcp1). The Argonaute protein Ago2 is a key element of the RNA-induced silencing complex (RISC), where microRNAs (miRNAs) and small interfering RNAs (siRNAs) bind to their mRNA targets to promote translational repression or mRNA decay (24, 25). GW182 is an RNA-binding protein that physically interacts with Argonautes and is required for miRNA-mediated silencing (26–28). Finally, the decapping coactivator Dcp1 is a classical marker of P bodies and promotes 5′-to-3′ degradation of deadenylated mRNA (29, 30).

In HeLa cells, transfected GFP-Ago2 and HA-GW182 primarily localized to cytoplasmic puncta. GFP-Ago2, CPEB3-DsRed, and HA-GW182 colocalized in cytoplasmic puncta identical to those of P bodies (Fig. 1*A*); over 70% of CPEB3-DsRed puncta colocalized with GFP-Ago2 and HA-GW182, while over 60% of GFP-Ago2 and HA-GW182 puncta colocalized with CPEB3-DsRed (*SI Appendix*, Fig. S1). We obtained similar results for Dcp1 (Fig. 1*B*).

To verify that P-body colocalization was not an artifact due to overexpression, we performed additional experiments to monitor localization of the endogenous proteins. We confirmed that both CPEB3-DsRed and endogenous CPEB3 colocalized with endogenous Ago2, Dcp1, and GW182 in P bodies (*SI Appendix*, Fig. S2). We repeated the immunofluorescence experiments in primary mouse hippocampal neuron cultures and confirmed that in the basal state the colocalization observed in HeLa cells resembles that in neurons (Fig. 1*C*). We next observed that CPEB3-DsRed colocalizes with the P-body markers Dcp1, GW182, and Ago2 (Fig. 1 *A*–*C*) but not with the stress granule marker TIA-1 (*SI Appendix*, Fig. S3). Thus, we find that CPEB3-DsRed localizes to P bodies in mouse hippocampal neurons and HeLa cells.

To determine whether CPEB3 interacts physically with components of the P body, we performed coimmunoprecipitations (co-IPs) on lysates of HEK 293T cells transfected with CPEB3. Because of their accessible morphology and resolution, we utilized HeLa cells in imaging studies. For biochemistry, we instead utilized HEK cells because they lack endogenous CPEB3, allowing us greater control over the CPEB3 in the system. Anti-GW182 antibody coimmunoprecipitated with CPEB3-EGFP; likewise, anti-GFP antibody coimmunoprecipitated GW182 with CPEB3-EGFP (Fig. 1*D*). Having established that CPEB3 interacts with GW182, we also tested CPEB3's interaction with Ago2. We were not able to immunoprecipitate CPEB3 with Ago2 using standard co-IP protocols, perhaps due to a lack of physical interaction or to a transient interaction that is difficult to capture by standard immunoprecipitation. Because P bodies are dynamic compartments, we decided to chemically cross-link the proteins in intact cells, in vivo, before performing coimmunoprecipitations to capture any transient interactions between CPEB3 and Ago2. In cross-linked samples, GFP-Ago2 and CPEB3-HA coimmunoprecipitated (Fig. 1*D*). Thus, our data suggest that CPEB3 resides in the same complexes with Ago2 and GW182. However, additional experiments are required to establish a direct physical interaction between CPEB3 and various P-body proteins.

RRM1 Is Necessary for the Interaction of CPEB3 with P-Body Components. To identify the domain(s) of interaction and to understand the functional relationship between CPEB3 and the components of the P body, we transfected HeLa cells with truncation mutants of CPEB3-GFP (Fig. 2). With the exception of the N-terminal domain, which does not contain any RNA binding site, each truncation mutant appeared in cytoplasmic puncta of different size and morphology, suggesting that the punctated granular appearance of CPEB3 might be driven by its association with mRNA or with other mRNA-binding proteins. In previous work from our laboratory, we also found that CPEB3 can self-associate due to the intermolecular interactions of its prion-like N terminus, which contains a putative coiled-coil domain (4, 8). This interaction appears to be unaffected by the presence of mRNA (4, 6). We further found that the RNA-binding domain also contributes to CPEB3 self-association,

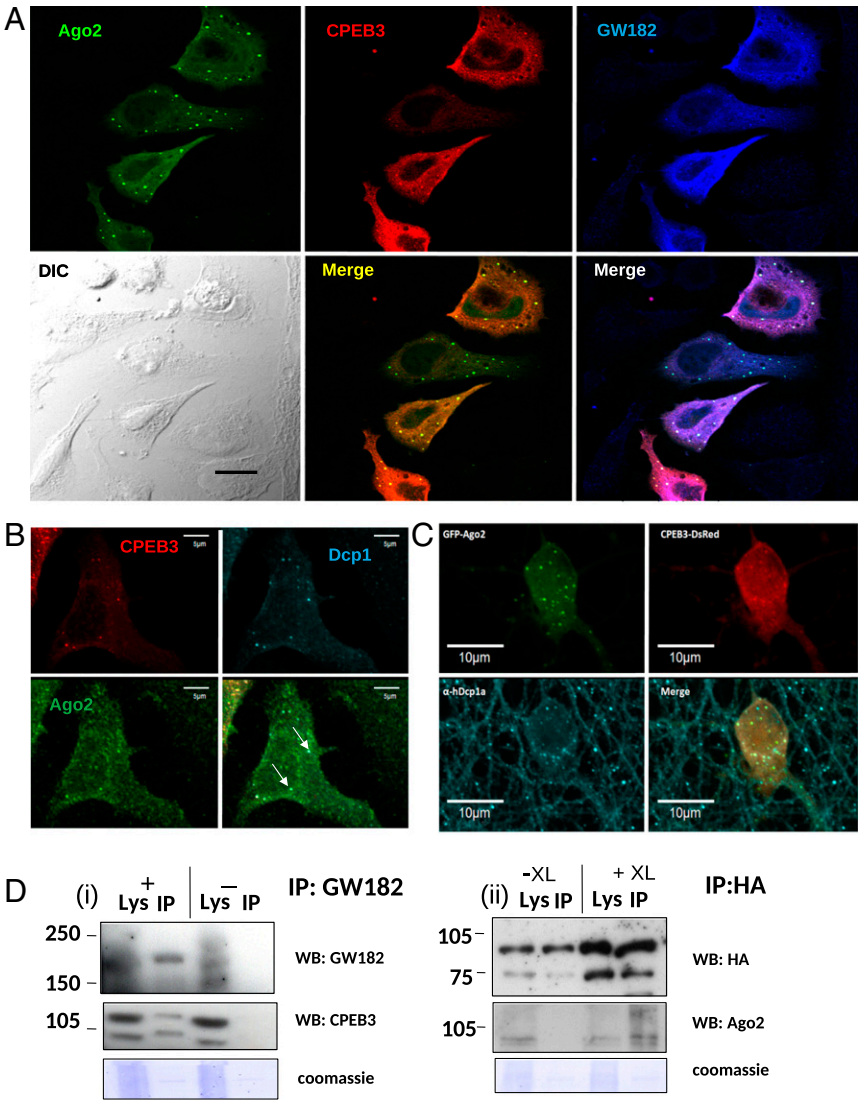

Fig. 1. CPEB3 colocalizes and interacts with P-body markers. (*A*) CPEB3-DsRed colocalizes with transfected P-body markers GFP-Ago2 (green) and HA-GW182 (blue) in HeLa cells. White puncta represent sites of CPEB3, Ago2, and GW182 colocalization. (Scale bar, 20 μm.) DIC, differential interference contrast. (*B*) CPEB3-DsRed colocalizes with endogenous P-body markers Dcp1 and Ago2. White puncta represent sites of CPEB3, Ago2, and Dcp1 colocalization and are distinguished with white arrows. (Scale bars, 5 μm.) (*C*) CPEB3-DsRed colocalizes with P-body markers in primary mouse hippocampal neurons. White puncta represent sites of CPEB3, Ago2, and Dcp1 colocalization. (Scale bars, 10 μm.) (*D*, *i*) Western blot of GW182 immunoprecipitation and HA immunoprecipitation from HEK 293T cells. IP, immunoprecipitated sample; Lys, cell lysate. In the GW182 immunoprecipitation blot, GW182 or CPEB3 was probed. (*D*, *ii*) Cross-linked, +XL; un–cross-linked, –XL. Western blot analysis of Ago2 and CPEB3 (HA) after immunoprecipitation. HA (for CPEB3) or Ago2 was probed. Representative Coomassie stains accompany appropriate blots.

although to a lesser extent than the N-terminal domain (4). Together, these data suggest that CPEB3 can form macromolecular assemblies thanks to the contribution of multiple domains (Fig. 2*A*). We next cotransfected each truncation mutant with GFP-Ago2 or HA-GW182 to observe any impairments in CPEB3's localization to P bodies. We found that CPEB3 does not require its N-terminal domain to enter P bodies since CPEB3ΔN-DsRed still colocalizes with GFP-Ago2 (Fig. 2*B*). Deletion of RRM2 also does not alter the localization to P bodies (Fig. 2*C*). The CPEB3ΔZnF-GFP mutant has a primarily nuclear distribution due to its lack of the NES; however, any remaining cytoplasmic CPEB3ΔZnF-GFP localizes to P bodies (Fig. 2*E*). On the other hand, deletion of CPEB3's RRM1 disrupts its colocalization with HA-Ago2 (Fig. 2*D*) and HA-GW182 (*SI Appendix*, Fig. S2), as their respective puncta do not colocalize but become juxtaposed to each other. Thus, RRM1 is necessary for CPEB3-GFP's colocalization with P-body components.

RRM1 Domain Is Necessary to Repress the Translation of CPEB3 mRNA Target GluA2. CPEB3 has been shown to repress translation of a reporter construct containing part of GluA2 mRNA (9) in neurons. Since P bodies are sites of translational repression or mRNA degradation, we wondered whether the localization of CPEB3 in P bodies is linked to its translational regulatory activity. To test this idea, we performed two sets of experiments.

First, we reasoned that if CPEB3 is indeed a major translational regulator of GluA2, we should be able to see a reduction in endogenous GluA2 protein in neurons transfected with wild-type CPEB3. As a control in our experiments, we overexpressed GFP alone, and verified that overexpression of GFP itself did not affect the basal levels of GluA2. We measured GluA2 protein levels when we transfected wild-type CPEB3-GFP in hippocampal neurons and found that overexpression of CPEB3 is followed by a significant reduction in the levels of GluA2. This is consistent with previous findings (4, 9, 10) that found a direct effect of CPEB3 on the translation of GluA2 mRNA by binding to its 3′ UTR.

Second, we tested the influence of P-body localization on the translational repression activity of CPEB3 by transfecting neurons with the ΔRRM1 mutant, which does not interact with P bodies. We measured the amount of GluA2 protein produced by transfected cells. We did not observe any reduction in the levels of GluA2, presumably reflecting a lack of repression of the translation of GluA2 mRNA (Fig. 3 *A* and *B*). To confirm our conclusions that changes in GluA2 levels are due to a direct effect of CPEB3 on GluA2 mRNA translation, we performed additional experiments in HeLa cells using a reporter construct

containing GluA2 3′ UTR (Fig. 3*C*) fused to DsRed. We transfected HeLa cells with DsRed alone, Globin 3′ UTR GFP, or GluA2 3′UTR DsRed, with or without CPEB3-HA. We found that in the absence of GluA2 UTR, DsRed protein levels were not affected by the presence of CPEB3. However, when we fused the 3′ UTR of GluA2 to DsRed, we found a significant reduction in the amount of translated protein when CPEB3 was cotransfected (Fig. 3*C*). In addition, we confirmed that localization to P bodies is important for CPEB3 to exert its repression of translation, since the ΔRRM1 mutant does not affect the translation of the reporter GluA2 3′ UTR. Together, these experiments allowed us to conclude that the RRM1 domain is necessary to repress the translation of CPEB3 mRNA targets.

Chemical Long-Term Potentiation Promotes the Translocation of CPEB3 from P Bodies to Polysomes. CPEB3 is found both in the nucleus and in the cytoplasm. Within the cytoplasm, CPEB3 distributes with other proteins that participate in the regulation of translation. When analyzed by differential centrifugation of cell extract, basal CPEB3 in neurons resided in fractions containing the P-body component Dcp1 and the deadenylase complex subunit CCR4 (*SI Appendix*, Fig. S1). This suggested that CPEB3 is mainly repressing or degrading its target mRNAs. Application of glutamate or other chemical long-term potentiation (cLTP)-inducing stimuli disrupts P bodies and promotes translation (15). Furthermore, CPEB3 is known to promote translation of its target mRNAs after LTP (4, 6). To fulfill this role, CPEB3 must move away from a degrading, P-body complex. To test whether this was the case, we evoked chemical LTP with forskolin and rolipram and observed CPEB3-expressing hippocampal neurons over time. We evaluated 5 time points: 0 min, 5 min, 15 min, 30 min, and 1 h poststimulation and tracked Dcp1- and CPEB3-colabeled puncta. We observed a significant decrease in CPEB3 and Dcp1 colocalization by the 30-min time point and saw an increase to baseline colocalization by 1 h in distal processes (Fig. 4). We noted a decrease in total Dcp1 and an increase in total CPEB3 over the time course, which has been previously observed under similar stimulation conditions (4, 15). We confirmed these results by Western blot analysis (*SI Appendix*, Fig. S4). We also established that the relatively fast increase in CPEB3 protein levels is due mainly to increased translation, since treatment with the translational inhibitor cycloheximide prevented the increase of CPEB3 protein levels (*SI Appendix*, Fig. S4).

We next fractionated extracts of cells that had been briefly stimulated with glutamate following the same procedure used in Fig. 1 (17) and found that a considerable amount of CPEB3 had become redistributed into the polysome fraction (Fig. 3*D*), thus confirming the idea that there is redistribution of CPEB3 following synaptic activity.

CPEB3 Undergoes Phase Separation In Vitro. To better understand the mechanism by which CPEB3 localizes to P bodies, we used a reductionist approach and produced phase-separated droplets in vitro. We produced recombinant CPEB3-HA in HEK 293T cells, immunoprecipitated CPEB3-HA via the HA tag, and separated it to high purity using size-exclusion chromatography (SEC) (Fig. 5 *A* and *B*). Under SEC conditions, CPEB3-HA elutes primarily in one sharp peak as a monomer (Fig. 5*B*). The recombinant CPEB3 was then examined under various conditions, such as changes in temperature, salt, metals, polyanions, molecular crowding agents, and posttranslational modifications, all of which have been observed to influence phase separation of other RNA-binding proteins (31–34). We had previously found that CPEB3 is small ubiquitin-like modifier (SUMO)ylated in its basal state and that it is de-SUMOylated after neuronal stimulation (5). We therefore first tested whether SUMO might affect the ability of CPEB3 to phase separate in vitro. Indeed, we found that CPEB3 undergoes phase separation in vitro when SUMOylated with SUMO1, SUMO2, and SUMO3, and when exposed to a specific mRNA target in an environment with molecular crowding agents (Fig. 5*C*). Phase separation was validated by measuring the turbidity of the sample, compared with an un-SUMOylated control. SUMOylated CPEB3 had a significant 15.1% ± 2.5 SEM increase in turbidity, compared across $n = 4$ samples with technical triplicates ($P < 0.001$). We used actin 3′ UTR as the specific RNA target in these experiments, to which CPEB3 binds under both basal and stimulating conditions (6). Temperature, salt, and metal did not have an obvious influence on phase separation of CPEB3, nor did general HeLa mRNA (*SI Appendix*, Fig. S5). The lack of general RNA influence on phase separation suggested that target mRNA binding is specific and necessary for phase separation. We then tested the influence of specific RNAs to induce phase separation of CPEB3 using an additional mRNA target of CPEB3, SUMO2 3′ UTR (5). Incubation of CPEB3 with SUMO2 3′ UTR induced phase separation, which caused a significant turbidity of the solution. However, a mutated SUMO2 3′ UTR, which prevents the binding of CPEB3 (5), did not induce phase separation (*SI Appendix*, Fig. S5). As a control for this technique, we subjected GFP alone to the same environmental conditions and did not find evidence of phase separation (*SI Appendix*, Fig. S5).

SUMOylation Drives CPEB3 Localization to P Bodies and Modulates the Ability of CPEB3 to Repress Translation of Its Target mRNAs. Thus far, our data suggest that in vivo CPEB3 is located in phase-separated RNA granules, such as P bodies. In vitro, we observed that CPEB3 phase separated when SUMOylated and bound to a specific target mRNA. To link the in vivo and in vitro findings, we utilized a CPEB3-GFP construct and ginkgolic acid treatment, which inhibits SUMOylation (35). When SUMOylation is inhibited, transfected CPEB3-GFP colocalizes less with the P-body marker Dcp1 (Fig. 5*D*). The ginkgolic acid studies suggest that SUMOylation is indeed important for CPEB3 colocalization to P bodies.

To further investigate the contribution of SUMOylation in modulating the activity of CPEB3, we used the reporter system previously described, containing GluA2 3′ UTR fused to DsRed. We transfected HeLa cells with DsRed GluA2 3′ UTR alone or in the presence of CPEB3 and SUMO. We found that changes in the amount of the reporter signal, analyzed by Western blot, are a direct consequence of its translation. We confirmed that, in the presence of CPEB3, the signal of the reporter is significantly reduced. Cotransfection with SUMO, which promotes phase separation of CPEB3 in vitro and modulates the colocalization of CPEB3 with P-body marker Dcp1 in cells, further reduces the expression of the reporter (Fig. 5*E*). Our data therefore suggest that SUMO plays a crucial role in mediating the activity of CPEB3 by mediating its distribution in P bodies.

Discussion

The RNA-binding protein CPEB3 mediates the translation of several identified mRNA targets (4, 9). However, the regulatory mechanism whereby CPEB3 mediates translation was previously not known. To gain insight into the function of CPEB3, we characterized its distribution in human cell lines and neuronal cultures. We found that CPEB3 leaves the nucleus by virtue of its nuclear export signal, and localizes to P bodies through its RNA recognition motif 1 in the cytoplasm, where it interacts with granular proteins Ago2 and GW182 and where mRNAs are known to be inhibited from translation (30). Furthermore, we find that SUMOylation of CPEB3 is critical for P-body localization and biophysical phase separation. When an appropriate stimulus is registered, CPEB3 leaves the P body and moves to the polysome, presumably to mediate the translation of its targets.

In the studies outlined above, we examined the cellular mechanism of CPEB3 function. We propose that CPEB3 acts as a translational inhibitor when it resides in P bodies, and following

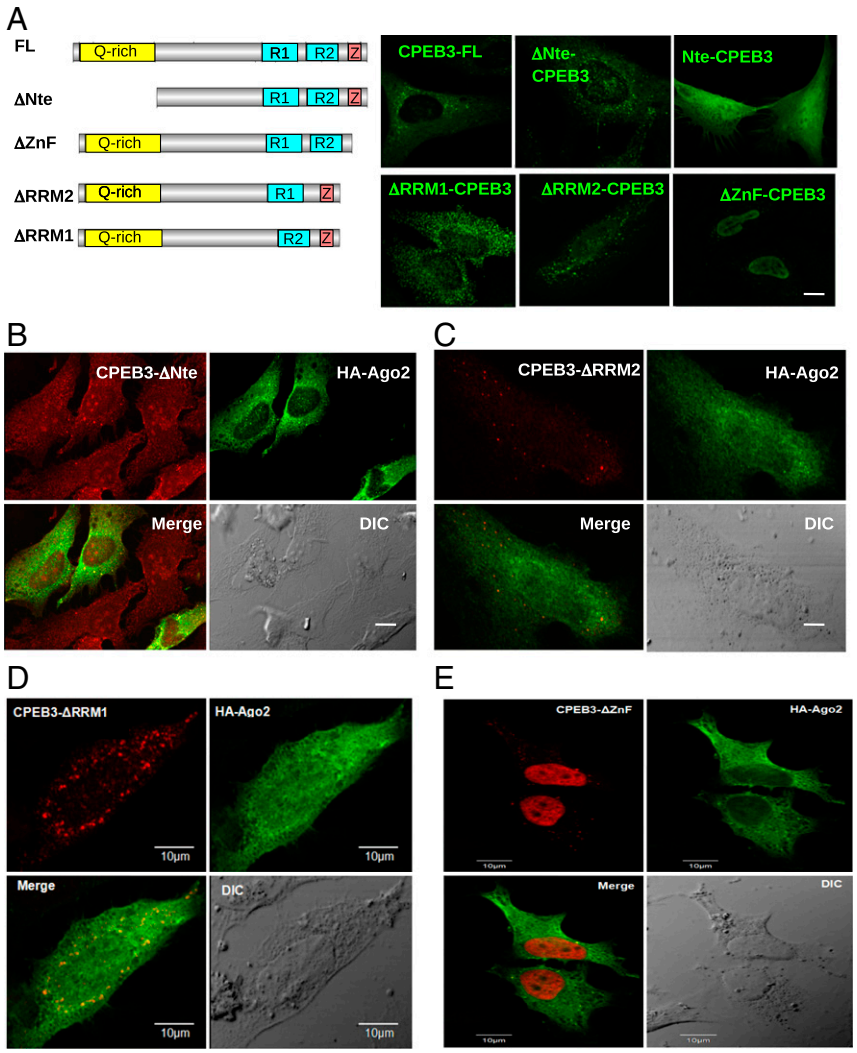

Fig. 2. RRM1 is required for CPEB3's localization to P bodies. (*A*) Schematic and representative HeLa cell expression images are indicated for each full-length or mutant CPEB3 sample used. (*B*) CPEB3 truncation mutant (red) without the N-terminal domain and P-body component Ago2 (green). (*C*) CPEB3 RRM2 deletion mutant (red) and P-body component Ago2 (green). (*D*) CPEB3 ZnF domain mutant (red) and P-body component Ago2 (green). (*E*) CPEB3 RRM1 domain mutant (red) and P-body component Ago2 (green). (Scale bars, 10 μm.)

specific stimuli (like synaptic stimulation in neurons) it moves away from them, promoting translation of the bound mRNAs.

Compartmentalization of proteins and RNA into P bodies and other RNA granules is extremely important for spatial and temporal regulation of cellular mechanisms. mRNAs that localize to P bodies undergo one of several fates, including degradation, nonsense-mediated decay, and RNA interference by siRNAs or miRNAs (30). The dynamics of RNA granules allows for specific entry and exit of different molecules, as well as for fusion or separation of various granules. These organelles allow for tight control over their contents. Indeed, this phenomenon appears to be important across many processes in cell biology, from nuclear membraneless bodies which house DNA and pre-mRNA splicing factors to cytosolic membraneless bodies which, along with the above-mentioned neuronal RNA granules, include germ granules (36).

In previous studies, our laboratory identified a structure–function link to CPEB3 translation activity. When inhibitory, CPEB3 is soluble, monomeric, and SUMOylated (4, 5). However, the promotional form of CPEB3, which is necessary for long-term memory maintenance, is insoluble and oligomeric (4). The findings of this paper, that CPEB3 is SUMOylated and inhibitory in the P body and then leaves the P body after cLTP to move into polysomes, strengthens previous structure–function findings. As stated above, P bodies provide a "holding cell" for mRNAs fated for degradation or translation. This ties in clearly with the stimulation dependence of CPEB3 translation activity. In addition, P body-bound proteins also appear to maintain highly dynamic structures and contain various available interaction sites, providing an important environment for controlling protein structure (37–40). This again ties in well with our understanding of the conformational dynamicity of CPEB3. Moreover, we draw further parallels between CPEB3 and P body-bound proteins cited in the literature.

First, phase separation of various proteins appears to be regulated, at least in part, by posttranslational modifications. Indeed, phosphorylation and dephosphorylation have been found to promote assembly and disassembly of membraneless organelles (32, 41–43). Intriguingly, phosphorylation of *Xenopus* and human CPEB4 regulates phase separation of the protein (44). There are examples of SUMOylation in the nucleus promoting the formation of membraneless PML nuclear bodies (45–47). In our study, we find that SUMOylation is important for phase separation of CPEB3-GFP in vitro and drives CPEB3 to P bodies in the cytoplasm of cells. The importance of posttranslational modifications in the phase separation of intrinsically disordered proteins cannot be understated. In fact, due to a lack of well-defined 3D structure, these proteins phase separate largely through availability of interaction sites in their low-complexity/disordered domains (37–40, 48). The orientation and availability of such interaction sites are altered with posttranslational modifications of key amino acid residues (48).

Second, specific mRNAs appear to drive phase separation in vitro. Many studies have observed that polyanions, including

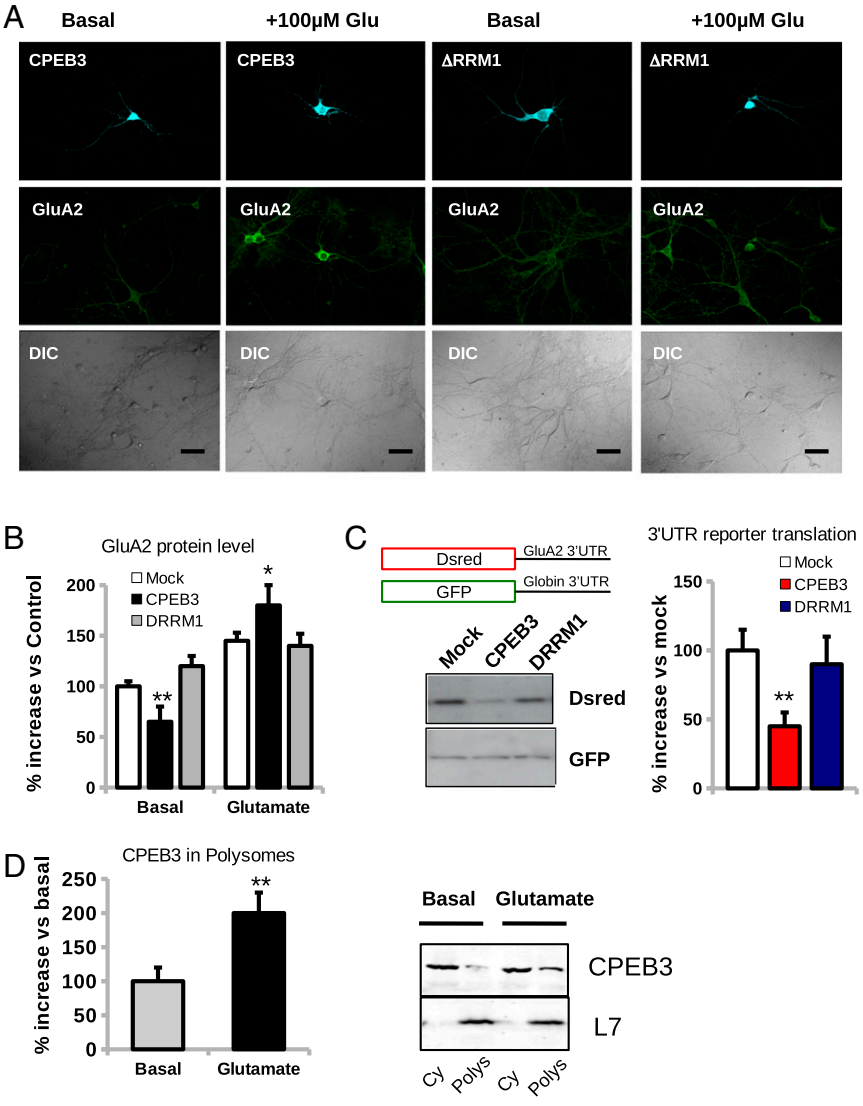

Fig. 3. RRM1 is required for CPEB3-mediated translation repression. (*A*) Hippocampal neurons were transfected with full-length CPEB3 and CPEB3ΔRRM1 (cyan) and the amount of GluA2 (green) was measured; 24 h after transfection, neurons were treated with vehicle or 100 μM glutamate for 2 min. (Scale bars, 10 μm.) (*B*) Quantification of glutamate-induced translation of GluA2. Full-length CPEB3 induces a statistically significant increase in GluA2 protein levels, while CPEB3ΔRRM1 does not differ from control, untransfected cells ($n = 12$ replicates per condition, ANOVA; $P < 0.01$, $^{*}P < 0.05$, $^{**}P < 0.01$, Tukey–Kramer post hoc analysis). Mock indicates transfection with empty vector. (*C*) Full-length CPEB3 or CPEB3ΔRRM1 was cotransfected with either DsRed-GluA2 3′ UTR or control GFP with an unrelated (hGlobin) 3′UTR. Significantly more DsRed was produced in the mock and CPEB3ΔRRM1 samples compared with samples expressing full-length CPEB3 ($n = 6$; ANOVA, with Tukey–Kramer post hoc analysis; $^{*}P < 0.05$, $^{**}P < 0.01$). (*D*) After stimulation, CPEB3 translocates to polysomes. Fractionation experiments show that glutamate stimulation induces a significant increase in the polysomal fraction. L7 is used as a marker of polysomes. Quantification of the amount of CPEB3 in the polysomal fraction ($n = 3$); *t* test reveals a significant difference ($^{**}P < 0.05$).

RNA, drive phase separation. Recently, others have verified that individual mRNAs drive phase separation, likely due to the secondary structure of the mRNA (49–51). Indeed, Zhang et al. (52) utilized the polyQ protein Whi3 and observed that RNA can specifically control phase separation of polyQ proteins. Interestingly, we also found that phase separation of polyQ-protein CPEB3 was mRNA-specific. Total HeLa mRNA was not able to drive phase separation. However, the CPEB3 mRNA target actin 3′ UTR (6) allowed for phase separation. Since actin 3′ UTR mRNA and Sumo2 3′ UTR were unable to drive phase separation with GFP, the CPEB3–mRNA complex appears to be critical for phase separation.

Finally, protein–protein interactions appear to influence the phase-separation processes. We believe that oligomeric CPEB3 is SUMOylated in P bodies and can either be degraded or move to the polysome upon stimulation, for mRNA target translation. Perhaps SUMOylation drives the formation of a supersecondary structure, such as a coiled-coil (8, 53, 54), creating low *n*-oligomers which phase separate and localize to RNA granules (33, 53, 55–57). This certainly appears to be a plausible cell biological regulatory mechanism, and fits in well with our understanding of the importance of the CPEB3 coiled-coil region (8). Indeed, one of the three nonmutually exclusive roles of SUMOylation is the conformational change of the SUMOylated substrate (58).

Understanding how cells regulate granular compartmentalization is critical for our understanding of local protein synthesis and for protein synthesis-dependent mechanisms, such as learning and memory. Our findings not only extend our basic understanding of the biology of the cell but also offer us new insights into healthy functioning of memory circuitry in the brain.

Materials and Methods

Mice. Mice were maintained under standard conditions, consistent with NIH guidelines and approved by the Institutional Animal Care and Use Committee of Columbia University.

Constructs. Available: CPEB3-EGFP, CPEB3-DsRed, CPEB3-HA, DsRed-N1, GluR2-short3′ UTR-DsRed, Globin 3′ UTR GFP, CPEB3-SUMO2-HA, SUMO1, SUMO2, SUMO3, and 3′-actin UTR.

Ordered: GFP-Ago2, HA-Ago2, and HA-GW182 from Addgene.

Software Prediction Using the *k*-NN Algorithm. We used the PSORT software available online at https://psort.hgc.jp/.

Subcellular Fractionation. Mouse hippocampal neuron lysates were fractionated as previously described (17).

All fractionation steps in Fig. 1 were carried out at 4 °C. Cells were disrupted by vacuum cavitation (200 psi for 10 min) in a buffer of 0.25 M sucrose, 50 mM Tris (pH 7.5), 25 mM KCl, 5 mM $MgCl_2$, 1 mM PMSF, and 1 μg/mL each aprotinin, pepstatin, and leupeptin (Sigma). The fractionation scheme

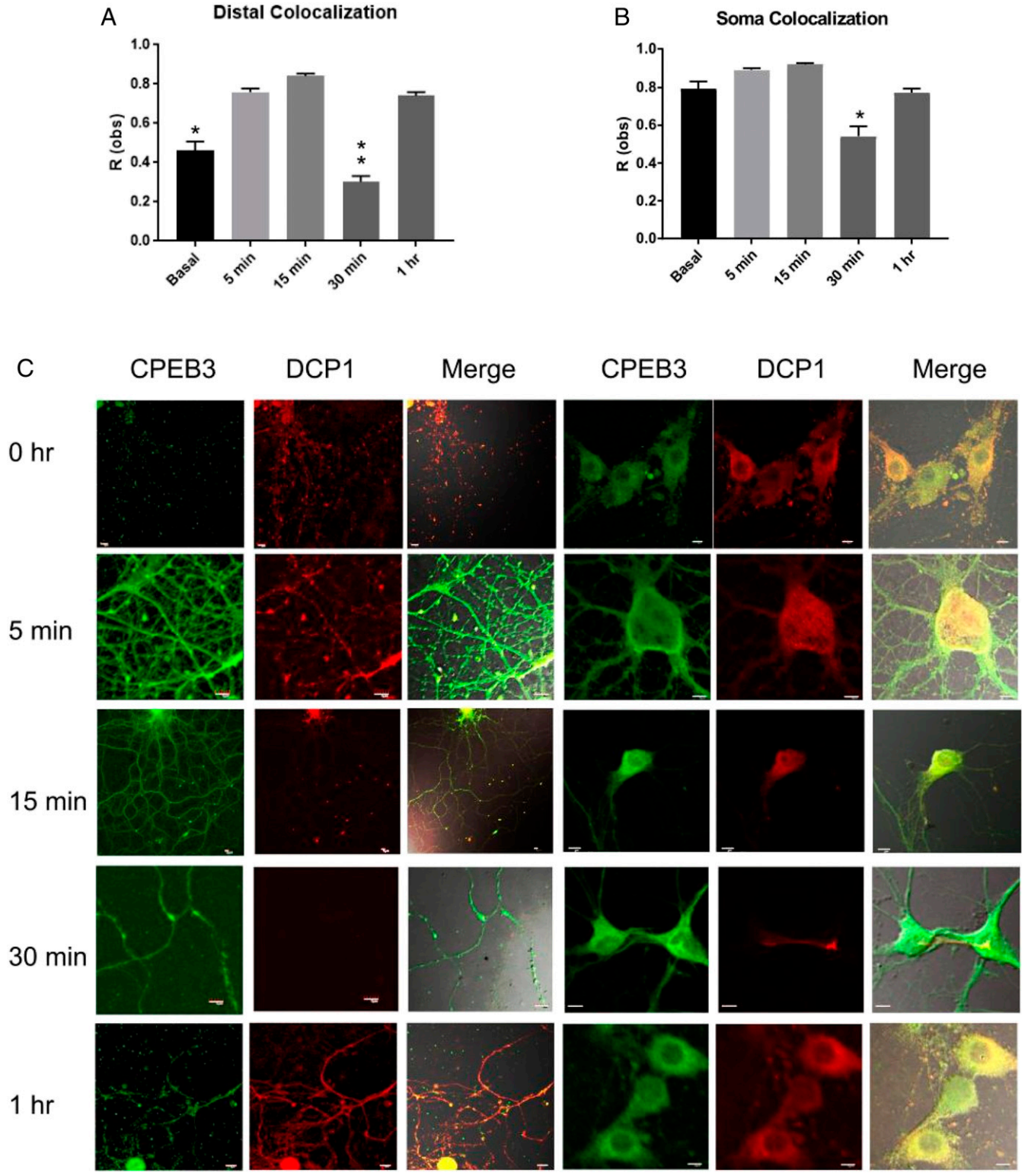

Fig. 4. CPEB3 localization to DCP1 decreases over time after cLTP stimulation. (*A*) Quantification of distal dendritic CPEB3 and Dcp1 colocalization over time, after cLTP stimulation. Asterisks indicate significance, $*P < 0.05$, $**P < 0.01$. One-way ANOVA and Tukey's multiple comparisons, with $n = 30$, 3 technical replicates. (*B*) Graphical representation of somatic CPEB3 and DCP1 colocalization over time, after cLTP stimulation. Asterisks indicate significance, $*P < 0.05$. One-way ANOVA and Tukey's multiple comparisons, with $n = 30$, 3 technical replicates. R(obs) represents the observed correlation of green and red signal, according to Fiji's colocalization test [which utilizes Costes's image randomization (100 iterations) and van Steensel and Fay's image shift analysis (62)]. (*C*) CPEB3 (green), DCP1 (red), or colocalization of the two (merge channel + DIC) at time points 0 h, 5 min, 15 min, 30 min, and 1 h after chemical long-term potentiation. Distal and somatic locales are represented. (Scale bars, 10 μm.).

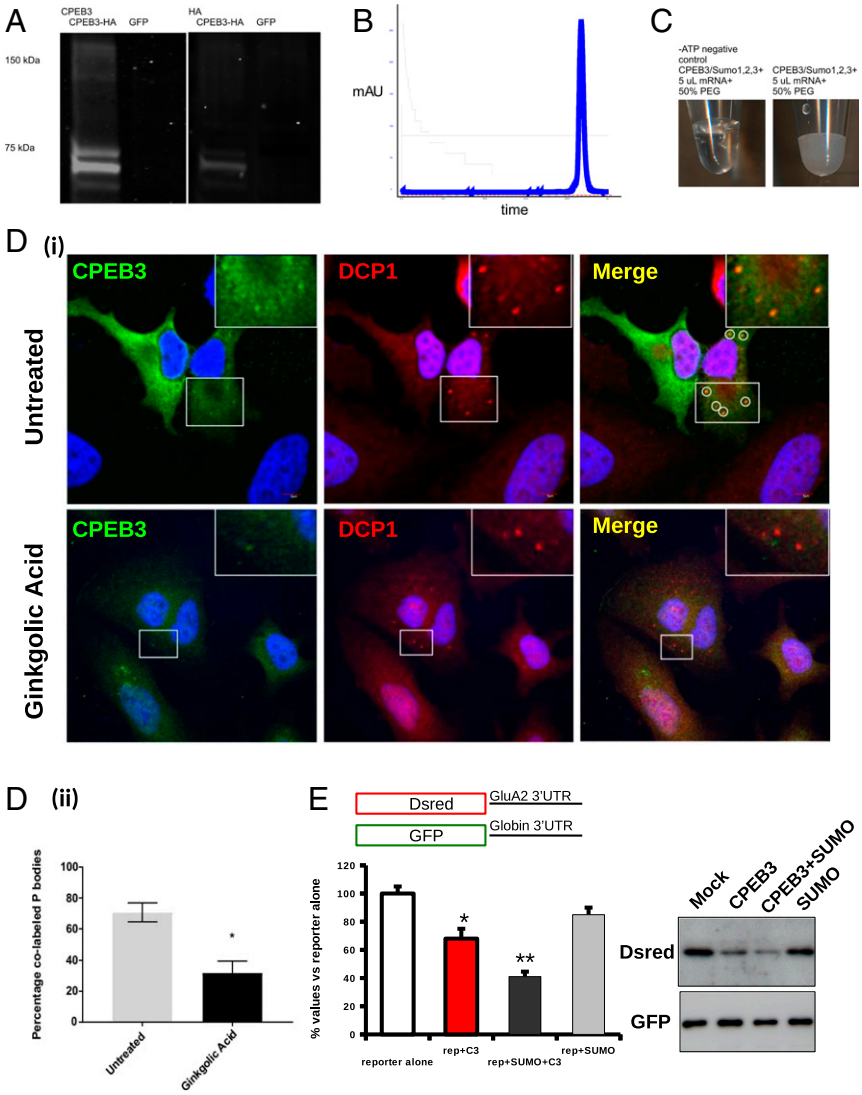

Fig. 5. SUMO mediates CPEB3 phase separation in vitro. (*A*) CPEB3-HA and GFP were overexpressed in HEK 293T cells and immunoprecipitated for HA. (*A*, *Left*) Western blot of CPEB3-HA and GFP eluates probed with CPEB3 antibody. (*A*, *Right*) HA probing. (*B*) Chromatogram from size-exclusion chromatography, with one sharp peak designating the protein fractions collected. (*C*, *Left*) ATP negative control of CPEB3/SUMO1, 2, 3 + 5 μL RNA + 50% PEG. (*C*, *Right*) Sample of CPEB3/SUMO1, 2, 3 + 5 μL RNA + 50% PEG. (*D*, *i*) HeLa cells transfected with CPEB3-GFP were treated with 100 μM ginkgolic acid for 6 h (CPEB3/ginkgolic acid) or treated with a sham (CPEB3/untreated). CPEB3-GFP is in green; P-body marker DCP1 is in red. Magnified inserts indicate areas of colocalization. (Scale bars, 10 μm.) (*D*, *ii*) Percentage of P bodies colabeled with CPEB3 in untreated ($n = 40$; across 5 sample groups) or ginkgolic acid-treated ($n = 23$; across 5 sample groups) samples. An asterisk represents statistical significance, $P = 0.0002$, *t* test. (*E*) DsRed GluA2 3′ UTR (reporter) alone, reporter + CPEB3, reporter + SUMO + CPEB3, or reporter + SUMO were expressed in cells. Cells were also transfected with GFP to control for transfection efficiency. Lysates were probed for DsRed and GFP. A significant reduction of DsRed production was observed when coexpressed with CPEB3. DsRed expression was further reduced when CPEB3 and SUMO were coexpressed ($*P < 0.05$, $**P < 0.001$, Tukey–Kramer post hoc analysis).

followed that of Krajewski (59). The lysate was subjected to 500 × *g* centrifugation for 5 min. The pellet was resuspended in 1.6 M sucrose and centrifuged through a 2.1 M sucrose pad at 150,000 × *g* for 1 h to isolate cytoplasm-free nuclei. The cytoplasmic supernatant was subjected to 10,000 × *g* centrifugation for 10 min to yield the heavy membrane pellet and the postnuclear supernatant. The postnuclear supernatant was then centrifuged for 1 h at 130,000 × *g*. The resulting pellet contained light membrane and polysomes, and the supernatant was centrifuged further at 180,000 × *g* for 3 h to yield the insoluble and soluble cytoplasmic fractions. All of the fractions were lysed in 1× Laemmli buffer containing 2% SDS and the protein concentration of each fraction was determined by Bradford assay (Bio-Rad).

Cell Culture. HEK 293 cells were cultured in Dulbecco's modified Eagle's medium with high glucose and L-glutamine (Gibco) with 10% FBS (Sigma) and 1% penicillin/streptomycin (Gibco) in a tissue-culture incubator at 37 °C and 5% CO_2. Cells were plated on 6-well flat-bottom cell-culture plates and grown to 70 to 80% confluency before transfection.

HeLa cells were cultured as described above and plated on 12-mm glass coverslips coated with poly–L-lysine (Sigma) in 24-well flat-bottom cell-culture plates. Cells were grown to 50 to 60% confluency before transfection. Leptomycin B (40 nM; Sigma; L2913) was applied to cells 24 h after transfection and incubated for 2 to 4 h.

Hippocampal cultures were obtained from P0 to P2 mouse pups as previously described (4) and plated on 24-well flat-bottom cell-culture plates with coverslips coated with poly–L-lysine (Sigma).

Transfection. HEK 293F and HeLa cells were transfected with TransFast Transfection Reagent (Promega) and 500 μg total DNA per 24-well culture dish or 2 μg total per 6-well culture dish. Cells were permitted to express plasmids for at least 18 h before performing experiments.

Neurons (10 d in vitro; DIV) were transfected with Lipofectamine LTX (Invitrogen) and 1 μg DNA per 2.0-cm^2 culture-plate well. Cells were permitted to express plasmids for at least 24 h before performing experiments.

Immunofluorescence. Cells were fixed with 4% paraformaldehyde and 5% sucrose in ice-cold PBS for 1 h, permeabilized for 2 min at room temperature (0.2% Triton-X in PBS), and blocked for 1 h at room temperature (5% FBS in PBS). For HeLa cells, coverslips were incubated overnight at 4 °C with primary antibody (Table 1) diluted in donkey or goat normal serum (Jackson Laboratory). For neurons, coverslips were coincubated for 3 h at room temperature with primary antibodies (Table 1). Coverslips were washed 3 times with PBS, incubated in fluorescent secondary antibody for 1 h at room temperature, and washed again in PBS. Coverslips were mounted using FluorSave Reagent (Calbiochem) and images were acquired on an Olympus IX81 laser-scanning confocal microscope using the FluoView FV1000 Microscopy System.

Immunoprecipitation of Transfected HEK 293 Cell Lysates. Cells were lysed in lysis buffer (10 mM Hepes, pH 7.4, 200 mM NaCl, 30 mM EDTA, 0.5% Triton-X, protease inhibitors [Roche], and 40 $U \cdot mL^{-1}$ RNasin), rotated at 4 °C for 20 min, and centrifuged for 5 min at 8,000 rpm. The supernatant was used for the IP as previously described (60) using protein A-Sepharose beads (Sigma), GW182 antibody (20 μg), and anti-mouse IgG as the negative control (20 μg; Santa Cruz). For HA IP: Cells were lysed in

Table 1. Antibodies

Antigen	Species	WB	IF	IP
Ago2 (2A8)	Mouse	1:1,000	1:400	–
CPEB3 (Abcam)	Rabbit	1:1,000	1:100	–
CPEB3 (08B1) homemade	Rabbit	1:2,000	1:200	1:20
HA (Covance)	Mouse	1:1,000	1:1,000	1:25
GFP (Clontech)	Mouse	–	–	1:25
GFP (G1)	Mouse	1:200	–	–
GW182 (4B6)	Mouse	1:1,000	1:100	2 μg
Anti-mouse HRP (Santa Cruz)	Donkey	1:10,000	–	–
Anti-rabbit HRP (Santa Cruz)	Donkey	1:10,000	–	–
Anti-mouse/rabbit 700 (LI-COR)	Donkey	1:15,000	–	–
Anti-mouse/rabbit 800 (LI-COR)	Donkey	1:15,000	–	–
Anti-mouse/rabbit Cy3 (Jackson Laboratory)	Goat	–	1:500	–
Anti-mouse/rabbit Cy5 (Jackson Laboratory)	Goat	–	1:500	–
Pumilio 1 (A300-201A; Bethyl)	Goat	–	1:1,000	
TIA-1 (Santa Cruz)	Goat	1:1,000	1:100	
CCR4 (Santa Cruz)	Rabbit	1:1,000	1:200	
FMRP (Millipore)	Mouse	1:2,000	1:200	
SUMO1 (Invitrogen)	Mouse	6 μL/mL	–	5 μg
SUMO2 (Invitrogen)	Rabbit	1/500	–	5 μg
SUMO3 (Life Technologies)	Rabbit	6 μL/mL	–	5 μg

IF, immunofluorescence; IP, immunoprecipitation; WB, Western blotting.

lysis buffer (10 mM Tris·HCl, pH 7.4, 0.5% Triton-X, protease inhibitors [Roche], and 100 μM PMSF), rotated at 4 °C for 20 min, and centrifuged for 5 min at 8,000 rpm. The supernatant was used for the IP as previously described (60) using HA-agarose beads (Sigma). Protein was natively eluted using HA peptide (Sigma) at 4 column volumes to 1 column volume of sample, or with Laemmli sample buffer for Western blot analysis.

Cross-Linking. Transfected HEK 293 cells were cross-linked as described previously (61) with the following modifications. Dithiobis(succinimidyl propionate) (DSP) (100×; 4 mg/mL) was prepared in DMSO and diluted to 2× DSP with PBS. Cells were washed twice with PBS and reincubated in PBS plus 1 volume of 2× DSP and left at room temperature for 5 min. Tris·HCl (pH 7.5; 100 μL) was added to a final concentration of 50 mM to quench DSP and left at room temperature for 5 min. The cells were scraped and centrifuged at 4 °C for 5 min at 4,000 rpm.

SDS/PAGE and Western Blotting.

Coomassie. TGX precast polyacrylamide gels (4 to 20%; Bio-Rad) were stained with GelCode Blue (Thermo) or transferred for Western blotting.

Chemiluminescence detection. IP samples were run on 8% SDS-polyacrylamide gels and transferred onto Immobilon PVDF membranes (Millipore). Membranes were blocked for 1 h in 5% milk in 0.1% TBS-T, washed 30 min in TBS-T, cut into pieces of appropriate size, and probed with primary antibody for 1 h at 4 °C. After extensive washing, membranes were probed for 1 h at room temperature with secondary antibody and washed. Blots were developed using SuperSignal West Dura Extended Duration Substrate (Pierce).

Fluorescence detection. IP samples were run on 8% SDS-polyacrylamide gels and transferred onto Immobilon-FL PVDF membranes (Millipore). Membranes were processed according to the manufacturer's protocol (LI-COR) and scanned using the Odyssey Infrared Imaging System with accompanying software.

Size-Exclusion Chromatography. Recombinant CPEB3-HA was further purified using gel filtration. A Superdex 200 column (GE Healthcare) was prepared with buffer A (50 mM Tris, pH 7.6, 20 mM NaCl, and 0.8 mM KCl); 500 μL recombinant CPEB3-HA eluate was injected. Sample and buffer A were flowed through the column using an AKTA Pure FPLC (GE Healthcare) at a flow rate of 0.5 mL/min. UNICORN 7.0 software (GE Healthcare) was used to monitor protein elution at 280 nm, and protein-containing fractions were collected using an automatic fraction collector (GE Healthcare). The presence of protein was verified by measuring the absorbance at 280 nm on a NanoDrop.

In Vitro Phase Separation. Purified recombinant CPEB3-HA was SUMOylated using a SUMOylation kit (Enzo Life Sciences) following the manufacturer's guidelines. Briefly, 4 μg CPEB3-HA was SUMOylated with human SUMO1, SUMO2, and SUMO3 in vitro with SUMO E1 enzyme, Ubc enzyme, and ATP + Mg^{2+}; 4 μg GFP was also SUMOylated as a protein control. SUMOylated CPEB3-HA (0.01 μg/μL) and GFP were exposed to various environmental conditions: room temperature or 4 °C; 2 M NaCl or physiological NaCl; 0.5 M ZnCl or no ZnCl; 3.2 μM actin-UTR RNA (6), 3.2 μM Sumo2-UTR RNA, 3.2 μM Sumo2 Mutant-UTR RNA, 3.2 μM total HeLa RNA (ThermoFisher), or no RNA; and 50% polyethylene glycol (PEG) or no PEG. Phase separation was observed qualitatively by the production of a gel-like substance. Phase separation was quantified using a turbidity assay. Using a NanoDrop, absorbance at 280 and 320 nm was measured across samples, in triplicate. An increase from baseline suggests an increase in particulate within the sample. Actin-UTR RNA was described previously (6). RNA was produced using the MAXIscript T7 Transcription Kit (Invitrogen) and further purified with RNA Clean and Concentrator (Zymo Research). Briefly, our actin-UTR construct (6) was transcribed to RNA using a T7 enzyme and appropriate dTPs. DNase removed non-RNA species, and column-based purification further cleaned the RNA before use in phase-separation studies.

Chemical Long-Term Potentiation. At 15 DIV, neurons were placed in fresh Neurobasal media for 3 min and then moved to stimulation media (50 μM forskolin, 0.1 μM rolipram, and 50 μM picrotoxin in ACSF without MgCl) for 5 min. Neurons were immediately moved back to their conditioned media and fixed in 4% PFA, 5% sucrose, PBS at either 0 h, 5 min, 15 min, 30 min, or 1 h.

Glutamate stimulation. At 15 DIV, neurons were also stimulated using a different protocol, a more general glutamatergic stimulation, using 100 μM glutamate for 2 min followed by washout at different time points. No signs of toxicity were evident up to several hours from stimulation. Neurons were also treated with actinomycin D (1 μg/mL) or cycloheximide (100 μM) in the presence of glutamate to establish what drives the increase of CPEB3 protein levels.

Ginkgolic Acid Treatment. HeLa cells were grown and transfected with CPEB3-GFP as discussed above. When cells had reached full expression, 100 μM ginkgolic acid in EtOH was added to each well and incubated for 6 h. To control for the addition of EtOH, "untreated" samples were treated with equal amounts of EtOH over the 6-h incubation. Immediately after incubation, cells were fixed and immunolabeled as discussed above.

Statistics. Statistical analyses were performed using GraphPad Prism 7. All data were analyzed using Student's *t* test or one-way ANOVA and Dunn's multiple comparison tests. Statistical significance was designated as $P < 0.05$.

ACKNOWLEDGMENTS. E.L. was supported by the Irene and Eric Simon Brain Research Foundation Summer Fellowship. We thank Peter Nelson for the anti-Ago2 (2A8) antibody and Jens Lykke-Andersen for the anti-hDcp1a antibody. We thank Cameron Parro for technical assistance. This work was supported by HHMI (E.R.K.).

1. A. Citri, R. C. Malenka, Synaptic plasticity: Multiple forms, functions, and mechanisms. *Neuropsychopharmacology* **33**, 18–41 (2008).
2. L. Wu *et al*., CPEB-mediated cytoplasmic polyadenylation and the regulation of experience-dependent translation of alpha-CaMKII mRNA at synapses. *Neuron* **21**, 1129–1139 (1998).
3. M. Theis, K. Si, E. R. Kandel, Two previously undescribed members of the mouse CPEB family of genes and their inducible expression in the principal cell layers of the hippocampus. *Proc. Natl. Acad. Sci. U.S.A.* **100**, 9602–9607 (2003).
4. L. Fioriti *et al*., The persistence of hippocampal-based memory requires protein synthesis mediated by the prion-like protein CPEB3. *Neuron* **86**, 1433–1448 (2015).
5. B. Drisaldi *et al*., SUMOylation is an inhibitory constraint that regulates the prion-like aggregation and activity of CPEB3. *Cell Rep.* **11**, 1694–1702 (2015).
6. J. S. Stephan *et al*., The CPEB3 protein is a functional prion that interacts with the actin cytoskeleton. *Cell Rep.* **11**, 1772–1785 (2015).
7. K. Si, S. Lindquist, E. R. Kandel, A neuronal isoform of the *Aplysia* CPEB has prion-like properties. *Cell* **115**, 879–891 (2003).
8. F. Fiumara, L. Fioriti, E. R. Kandel, W. A. Hendrickson, Essential role of coiled coils for aggregation and activity of Q/N-rich prions and polyQ proteins. *Cell* **143**, 1121–1135 (2010).
9. Y. S. Huang, M. C. Kan, C. L. Lin, J. D. Richter, CPEB3 and CPEB4 in neurons: Analysis of RNA-binding specificity and translational control of AMPA receptor GluR2 mRNA. *EMBO J.* **25**, 4865–4876 (2006).
10. E. Pavlopoulos *et al*., Neuralized1 activates CPEB3: A function for nonproteolytic ubiquitin in synaptic plasticity and memory storage. *Cell* **147**, 1369–1383 (2011).
11. W. H. Huang, H. W. Chao, L. Y. Tsai, M. H. Chung, Y. S. Huang, Elevated activation of CaMKIIα in the CPEB3-knockout hippocampus impairs a specific form of NMDAR-dependent synaptic depotentiation. *Front. Cell. Neurosci.* **8**, 367 (2014).
12. L. Groc, D. Choquet, AMPA and NMDA glutamate receptor trafficking: Multiple roads for reaching and leaving the synapse. *Cell Tissue Res.* **326**, 423–438 (2006).
13. H. W. Kessels, R. Malinow, Synaptic AMPA receptor plasticity and behavior. *Neuron* **61**, 340–350 (2009).
14. J. M. Henley, E. A. Barker, O. O. Glebov, Routes, destinations and delays: Recent advances in AMPA receptor trafficking. *Trends Neurosci.* **34**, 258–268 (2011).
15. N. Cougot *et al*., Dendrites of mammalian neurons contain specialized P-body-like structures that respond to neuronal activation. *J. Neurosci.* **51**, 13793–13804 (2008).
16. X. P. Wang, N. G. F. Cooper, Characterization of the transcripts and protein isoforms for cytoplasmic polyadenylation element binding protein-3 (CPEB3) in the mouse retina. *BMC Mol. Biol.* **10**, 109 (2009).
17. Y. Feng *et al*., Fragile X mental retardation protein: Nucleocytoplasmic shuttling and association with somatodendritic ribosomes. *J. Neurosci.* **17**, 1539–1547 (1997).
18. C. Temme, S. Zaessinger, S. Meyer, M. Simonelig, E. Wahle, A complex containing the CCR4 and CAF1 proteins is involved in mRNA deadenylation in *Drosophila*. *EMBO J.* **23**, 2862–2871 (2004).
19. R. Doidge, S. Mittal, A. Aslam, G. S. Winkler, Deadenylation of cytoplasmic mRNA by the mammalian Ccr4-Not complex. *Biochem. Soc. Trans.* **40**, 896–901 (2012).
20. P. Rojas-Ríos *et al*., Translational control of autophagy by Orb in the *Drosophila* germline. *Dev. Cell* **35**, 622–631 (2015).
21. Q. Sun, *et al*., Nuclear export inhibition through covalent conjugation and hydrolysis of leptomycin B by CRM1. *Proc. Natl. Acad. Sci. U.S.A.* **110**, 1303–1308 (2013).
22. H. W. Chao *et al*., NMDAR signaling facilitates the IPO5-mediated nuclear import of CPEB3. *Nucleic Acids Res.* **40**, 8484–8498 (2012).
23. P. Anderson, N. Kedersha, RNA granules. *J. Cell Biol.* **172**, 803–808 (2006).
24. G. L. Sen, H. M. Blau, Argonaute 2/RISC resides in sites of mammalian mRNA decay known as cytoplasmic bodies. *Nat. Cell Biol.* **7**, 633–636 (2005).
25. J. Liu, M. A. Valencia-Sanchez, G. J. Hannon, R. Parker, MicroRNA-dependent localization of targeted mRNAs to mammalian P-bodies. *Nat. Cell Biol.* **7**, 719–723 (2005).
26. J. Liu *et al*., A role for the P-body component GW182 in microRNA function. *Nat. Cell Biol.* **7**, 1261–1266 (2005).
27. S. L. Lian *et al*., The C-terminal half of human Ago2 binds to multiple GW-rich regions of GW182 and requires GW182 to mediate silencing. *RNA* **15**, 804–813 (2009).
28. K. Takimoto, M. Wakiyama, S. Yokoyama, Mammalian GW182 contains multiple Argonaute-binding sites and functions in microRNA-mediated translational repression. *RNA* **15**, 1078–1089 (2009).
29. U. Sheth, R. Parker, Decapping and decay of messenger RNA occur in cytoplasmic processing bodies. *Science* **300**, 805–808 (2003).
30. A. Eulalio, I. Behm-Ansmant, E. Izaurralde, P bodies: At the crossroads of post-transcriptional pathways. *Nat. Rev. Mol. Cell Biol.* **8**, 9–22 (2007).
31. J. T. Wang *et al*., Regulation of RNA granule dynamics by phosphorylation of serine-rich, intrinsically disordered proteins in *C. elegans*. *eLife* **3**, e04591 (2014).
32. I. Kwon *et al*., Phosphorylation-regulated binding of RNA polymerase II to fibrous polymers of low-complexity domains. *Cell* **155**, 1049–1060 (2013).
33. A. H. Fox, C. S. Bond, A. I. Lamond, P54nrb forms a heterodimer with PSP1 that localizes to paraspeckles in an RNA-dependent manner. *Mol. Biol. Cell* **16**, 5304–5315 (2005).
34. J. B. Rayman, K. A. Karl, E. R. Kandel, TIA-1 self-multimerization, phase separation, and recruitment into stress granules are dynamically regulated by Zn^{2+}. *Cell Rep.* **22**, 59–71 (2018).
35. I. Fukuda *et al*., Ginkgolic acid inhibits protein SUMOylation by blocking formation of the E1-SUMO intermediate. *Chem. Biol.* **16**, 133–140 (2009).
36. D. M. Mitrea, R. W. Kriwacki, Phase separation in biology; functional organization of a higher order. *Cell Commun. Signal.* **14**, 1 (2016).
37. S. Elbaum-Garfinkle *et al*., The disordered P granule protein LAF-1 drives phase separation into droplets with tunable viscosity and dynamics. *Proc. Natl. Acad. Sci. U.S.A.* **112**, 7189–7194 (2015).
38. M. Feric *et al*., Coexisting liquid phases underlie nucleolar subcompartments. *Cell* **165**, 1686–1697 (2016).
39. T. J. Nott *et al*., Phase transition of a disordered nuage protein generates environmentally responsive membraneless organelles. *Mol. Cell* **57**, 936–947 (2015).
40. K. A. Burke, A. M. Janke, C. L. Rhine, N. L. Fawzi, Residue-by-residue view of in vitro FUS granules that bind the C-terminal domain of RNA polymerase II. *Mol. Cell* **60**, 231–241 (2015).
41. P. Li *et al*., Phase transitions in the assembly of multivalent signalling proteins. *Nature* **483**, 336–340 (2012).
42. D. T. Murray *et al*., Structure of FUS protein fibrils and its relevance to self-assembly and phase separation of low-complexity domains. *Cell* **171**, 615–627.e16 (2017).
43. T. W. Han *et al*., Cell-free formation of RNA granules: Bound RNAs identify features and components of cellular assemblies. *Cell* **149**, 768–779 (2012).
44. J. Guillén-Boixet, V. Buzon, X. Salvatella, R. Méndez, CPEB4 is regulated during cell cycle by ERK2/Cdk1-mediated phosphorylation and its assembly into liquid-like droplets. *eLife* **5**, e19298 (2016).
45. T. H. Shen, H. K. Lin, P. P. Scaglioni, T. M. Yung, P. P. Pandolfi, The mechanisms of PML-nuclear body formation. *Mol. Cell* **24**, 331–339 (2006).
46. G. Dellaire, R. W. Ching, H. Dehghani, Y. Ren, D. P. Bazett-Jones, The number of PML nuclear bodies increases in early S phase by a fission mechanism. *J. Cell Sci.* **119**, 1026–1033 (2006).
47. S. F. Banani *et al*., Compositional control of phase-separated cellular bodies. *Cell* **166**, 651–663 (2016).
48. P. St George-Hyslop *et al*., The physiological and pathological biophysics of phase separation and gelation of RNA binding proteins in amyotrophic lateral sclerosis and fronto-temporal lobar degeneration. *Brain Res.* **1693**, 11–23 (2018).
49. B. Van Treeck *et al*., RNA self-assembly contributes to stress granule formation and defining the stress granule transcriptome. *Proc. Natl. Acad. Sci. U.S.A.* **115**, 2734–2739 (2018).
50. E. M. Langdon *et al*., mRNA structure determines specificity of a polyQ-driven phase separation. *Science* **360**, 922–927 (2018).
51. S. Maharana *et al*., RNA buffers the phase separation behavior of prion-like RNA binding proteins. *Science* **360**, 918–921 (2018).
52. H. Zhang *et al*., RNA controls polyQ protein phase transitions. *Mol. Cell* **60**, 220–230 (2015).
53. M. Zeng *et al*., Phase transition in postsynaptic densities underlies formation of synaptic complexes and synaptic plasticity. *Cell* **166**, 1163–1175.e12 (2016).
54. J. B. Woodruff *et al*., The centrosome is a selective condensate that nucleates microtubules by concentrating tubulin. *Cell* **169**, 1066–1077.e10 (2017).
55. X. Zhang *et al*., RNA stores tau reversibly in complex coacervates. *PLoS Biol.* **15**, e2002183 (2017).
56. B. E. Zucconi *et al*., Alternatively expressed domains of AU-rich element RNA-binding protein 1 (AUF1) regulate RNA-binding affinity, RNA-induced protein oligomerization, and the local conformation of bound RNA ligands. *J. Biol. Chem.* **285**, 39127–39139 (2010).
57. H. L. Okunola, A. R. Krainer, Cooperative-binding and splicing-repressive properties of hnRNP A1. *Mol. Cell. Biol.* **29**, 5620–5631 (2009).
58. K. A. Wilkinson, J. M. Henley, Mechanisms, regulation and consequences of protein SUMOylation. *Biochem. J.* **428**, 133–145 (2010).
59. S. Krajewski *et al*., Investigation of the subcellular distribution of the bcl-2 oncoprotein: Residence in the nuclear envelope, endoplasmic reticulum, and outer mitochondrial membranes. *Cancer Res.* **53**, 4701–4714 (1993).
60. T. Peritz *et al*., Immunoprecipitation of mRNA-protein complexes. *Nat. Protoc.* **1**, 577–580 (2006).
61. M. Wyszynski *et al*., Interaction between GRIP and liprin-alpha/SYD2 is required for AMPA receptor targeting. *Neuron* **34**, 39–52 (2002).
62. K. W. Dunn, M. M. Kamocka, J. H. McDonald, A practical guide to evaluating colocalization in biological microscopy. *Am. J. Physiol. Cell Physiol.* **300**, C723–C742 (2011).